

UNIVERSIDADE ESTADUAL DE CAMPINAS  
SISTEMA DE BIBLIOTECAS DA UNICAMP  
REPOSITÓRIO DA PRODUÇÃO CIENTÍFICA E INTELLECTUAL DA UNICAMP

**Versão do arquivo anexado / Version of attached file:**

Versão do Editor / Published Version

**Mais informações no site da editora / Further information on publisher's website:**

<https://journals.sagepub.com/doi/10.1366/11-06260>

**DOI: 10.1366/11-06260**

**Direitos autorais / Publisher's copyright statement:**

©2012 by Sage. All rights reserved.

DIRETORIA DE TRATAMENTO DA INFORMAÇÃO

Cidade Universitária Zeferino Vaz Barão Geraldo

CEP 13083-970 – Campinas SP

Fone: (19) 3521-6493

<http://www.repositorio.unicamp.br>

# Effects of Etching on Zircon Grains and Its Implications for the Fission Track Method

CARLOS ALBERTO TELLO SÁENZ,\* EDUARDO AUGUSTO CAMPOS CURVO, AIRTON NATANAEL COELHO DIAS, CLEBER JOSÉ SOARES, CARLOS JOSÉ LEOPOLDO CONSTANTINO, IGOR ALENCAR, SANDRO GUEDES, ROSANE PALISSARI, and JULIO CESAR HADLER NETO

*Departamento de Física Química e Biologia, UNESP Universidade Estadual Paulista, 19060-900 Presidente Prudente, SP, Brazil (C.A.T.S., E.A.C.C., A.N.C.D., C.J.L.C.); Instituto de Geociências e Ciências Exatas, UNESP Universidade Estadual Paulista, 13506-900, Rio Claro, SP, Brazil (C.J.S.); and Instituto de Física “Gleb Wataghin”, Universidade Estadual de Campinas, UNICAMP, 13083-970 Campinas, SP, Brazil (I.A., S.G., R.P., J.C.H.N.)*

Studies of zircon grains using optical microscopy, micro-Raman spectroscopy, and scanning electron microscopy (SEM) have been carried out to characterize the surface of natural zircon as a function of etching time. According to the surface characteristics observed using an optical microscope after etching, the zircon grains were classified as: (i) homogeneous; (ii) anomalous, and (iii) hybrid. Micro-Raman results showed that, as etching time increases, the crystal lattice is slightly altered for *homogeneous* grains, it is completely damaged for *anomalous* grains, and it is altered in some areas for *hybrid* grains. The SEM (energy dispersive X-ray spectroscopy, EDS) results indicated that, independent of the grain types, where the crystallinity remains after etching, the chemical composition of zircon is approximately 33% SiO<sub>2</sub>:65% ZrO<sub>2</sub> (standard natural zircon), and for areas where the grain does not have a crystalline structure, there are variations of ZrO<sub>2</sub> and, mainly, SiO<sub>2</sub>. In addition, it is possible to observe a uniform surface density of fission tracks in grain areas where the determined crystal lattice and chemical composition are those of zircon. Regarding hybrid grains, we discuss whether the areas slightly altered by the chemical etching can be analyzed by the fission track method (FTM) or not. Results of zircon fission track and U-Pb dating show that hybrid and homogeneous grains can be used for dating, and not only homogeneous grains. More than 50 sedimentary samples from the Bauru Basin (southeast Brazil) were analyzed and show that only a small amount of grains are homogeneous (10%), questioning the validity of the rest of the grains for thermo-chronological evolution studies using zircon FTM dating.

Index Headings: Zircon; Micro-Raman spectroscopy; Fission track method; Scanning electron microscopy; SEM; Energy dispersive X-ray spectroscopy; EDS; Zircon crystal lattice; Zircon chemical etching.

## INTRODUCTION

The fission track method, FTM, is commonly used to evaluate thermo-chronological evolution in regions of geological interest. This application is based on the accumulation of fission tracks, originating from spontaneous fission decay of <sup>238</sup>U on the geological time scale, and the possibility that these tracks can be revealed when a mineral is submitted to appropriate etching. Some minerals to which FTM is commonly applied include, for instance, apatite and zircon, whose principal difference is the range of temperatures in which fission tracks have their lengths partially shortened (partial annealing zone, PAZ). Thus, from the measurement of fission track lengths it is possible to infer the interval of time

over which the mineral experienced PAZ temperatures and then reconstruct its geological thermal history. In the case of apatite, the PAZ spans between 60 and 110 °C (considering the time period of 1 Ma, where Ma is “million years”). The same interval is required for maturation of hydrocarbons in Ma (see Gallagher et al.<sup>1</sup> and references therein). For zircon, the PAZ spans between 190 and 380 °C (for heating durations of 1 Ma).<sup>2</sup> In this way, zircon enables the study of more intense thermal events and/or to find the crystallization age. An important example of its application is the geological fault dated by Murakami et al.<sup>3</sup> Thus, zircon fission track analysis complements the information given by the apatite fission track analysis.

Depending on the sample, laboratory treatments of zircon may be very laborious, reflecting the scarce annealing data previously presented.<sup>4–6</sup> However, it is possible to use this data for annealing modeling (e.g., Guedes et al.<sup>7</sup>). One of the major issues in the application of FTM to zircon is the track etching.<sup>8</sup> Etching and annealing (track fading by temperature<sup>9</sup>) of fission tracks in zircon are affected by: (i) crystallization through magmatic or metamorphic zonation; (ii) metamictization (partial or total damage of the crystal lattice caused by nuclide recoil during alpha decay) when the mineral has high concentration of uranium (U) and thorium (Th) (above 5000 ppm of UO<sub>2</sub> + ThO<sub>2</sub>),<sup>10,11</sup> and (iii) the incorporation of other minerals. Such events can take place in zircons of igneous or detrital rocks. In general, at least one of these phenomena can be identified in natural zircons.

Over the last decade, micro-Raman spectroscopy has been applied to zircon to analyze radiation effects in the annealing process. Micro-Raman spectroscopy data present systematic changes in frequency, relative intensity, and/or band width according to the dose. These data are related to metamictization,<sup>11–15</sup> i.e., the loss of the periodic crystal structure. This phenomenon is the result of the accumulation of radiation damage over time in the geological timescale.<sup>16</sup> In natural zircons, metamictization is the result of the radioactive decay of U and Th incorporated during crystal growth (as well as the decay of their daughter products) and, therefore, the crystallization degree in a zircon sample may be described by the relative amounts of the amorphous and swelled crystalline fractions. According to Wasilewski et al.<sup>17</sup> and other researchers,<sup>18–20</sup> the  $\alpha$ -recoil nuclei directly amorphize the structure, whereas point defects created by particles, together with the tangent stress from adjacent amorphous regions, induce swelling of the crystal structure. Palenik et al.<sup>11</sup> presented a micro-analytic study (optical microscopy, Raman spectroscopy, and

Received 9 February 2011; accepted 23 January 2012.

\* Author to whom correspondence should be sent. E-mail: tello@fct.unesp.br.

DOI: 10.1366/11-06260

high-resolution transmission electron microscopy (HR-TEM)) of a zircon from Sri Lanka (alluvial zircon, with an estimated age of  $570 \pm 20$  Ma), in which they observed zoning resulting from radiation damage (see also Chakoumakos et al.<sup>21</sup>). Evidence for the increased reactivity of metamict zircon is also given by the discordant ages determined from metamict areas of natural zircon samples.<sup>22–24</sup> However, little attention has been paid to the role of metamictization on the chemical stability of zircon at the Earth's surface.<sup>25</sup> Also, little is known about the effect of chemical etching over the zircon crystal lattice.

In the present work, the study of natural zircon surfaces was carried out using micro-Raman spectroscopy as a function of etching time. For this goal, we used a sample, denoted JP, collected in the Barreiras Formation, near the city of Mataraca, State of Paraíba, northeast Brazil. The Barreiras Formation is a continental sedimentary deposit along the Brazilian coastline spanning from the State of Rio de Janeiro to the State of Amapá.<sup>26</sup> These detrital zircons present a mean uranium content of 130 ppm (calculated via neutron irradiation against standard uranium doped glasses) and mean Th/U ratio of 0.7 (calculated from inductively coupled plasma mass spectrometry (ICP-MS) measurements). The scanning electronic microscopy, SEM (energy dispersive spectroscopy (EDS)), was also used to characterize the zircon surface and to estimate the concentration of its main chemical oxide elements ( $ZrO_2$  and  $SiO_2$ ). Three types of zircon grains were identified after etching according to their response. They were classified here as *homogeneous*, *anomalous*, and *hybrid* grains. The aim of this work is to check the possibility of using *hybrid* grains in FTM. As a result, eight grains (*homogeneous* and *hybrid*) were dated by FTM and U-Pb dating to show that these zircon grains can be indeed used in thermo-geochronology. This work is complementary to the one carried out for *heterogeneous* grains, which show non-uniform fission-track distribution.<sup>27</sup>

## EXPERIMENTAL PROCEDURES

The characterization of zircon grains was carried out before and after etching in terms of their surface morphology (optical microscopy) and crystalline structure (micro-Raman spectroscopy). Determination of the main chemical oxide elements (SEM/EDS) was carried out only after the etching. Optical microscopy and micro-Raman spectroscopy analyses were done for samples with no etching or with 6, 12, and 18 hours of etching. The experimental procedure for standard etching is described by Tagami et al.<sup>5</sup> Etching took place in steps until surface tracks perpendicular to the crystallography C-axis reach approximately  $2 \mu\text{m}$  width.<sup>4</sup> The ideal etching time for samples used in this work was 18 hours. The SEM (EDS) analyses were carried out only for 18 hours of etching. The optical microscopy images were recorded using a microscope Leica DMRX, with nominal magnification up to  $1500\times$ , digital camera (ExwaveHAD Sony, model SSC-DC54A), and Image-Pro Plus 4.0 program for image acquisition. After etching, it shows that (i) a typical *homogeneous* grain surface has its crystallinity slightly changed after the chemical etching and presents a uniform fission-track distribution; (ii) an *anomalous* grain surface loses the crystallinity presented before etching, being heavily etching damaged. This etching damage may be occurring due to several physicochemical phenomena, and not only due to metamictization. Another possibility is the incorporation of other minerals;<sup>28</sup> and (iii) a *hybrid* grain surface presents preserved areas (with crystallinity and fission

tracks, as in the homogeneous grain case) and damaged areas (as in the anomalous grain case). The zircon classification used in this work tries to describe an etched surface characteristic, which may be well known in the fission track community but has not yet been reported. We could call the *hybrid* grain (for instance) a “patchily over-etched” grain, but this classification implies that one area reveals tracks and another does not. However, this is typical of grains that present etching anisotropy, which is not the case here. The *hybrid* grain maintains (after etching) areas with tracks while other areas are completely damaged by the etching.

Micro-Raman spectroscopy was carried out using a spectrograph micro-Raman Renishaw model in-Via equipped with a charge-coupled device (CCD) detector, Leica Microscope, lasers at 514.5, 633, and 785 nm, an automatic sample holder base (which allows X, Y, and Z translations with steps of  $0.1 \mu\text{m}$ ), and gratings with 1800 and 1200 grooves/mm. The Raman spectra were collected with spatial resolution around  $1 \mu\text{m}^2$ , spectral resolution of approximately  $2.5 \text{ cm}^{-1}$ , and directly from the grains without any further treatment beyond the one necessary for the fission track analysis (i.e., polishing and etching). The measurements were done with the 514.5 nm laser line focused perpendicular to the C-axis using the  $50\times$  objective lens and gratings with 1200 grooves/mm. The SEM (EDS) measurements<sup>29</sup> were performed with a scanning electron microscope LEO430. The electron beam operated with energy of 20 keV, working distance of 19 mm, beam current of  $3 \times 10^{-9}$  A, and vacuum of  $1 \times 10^{-5}$  torr. Samples were coated with carbon before measurement to avoid charge effects. The process to obtain grains of zircon utilized conventional techniques, i.e., by crushing, grinding, magnetic, and heavy liquid separations. After these, zircon grains were mounted in a sheet of Teflon PFA and polished. Before etching, all grains were observed by optical microscopy and presented a flat surface from characteristic zircon grains. The etching was done with an eutectic mixture of KOH:NaOH at  $(225 \pm 2)^\circ \text{C}$ .<sup>8,30</sup>

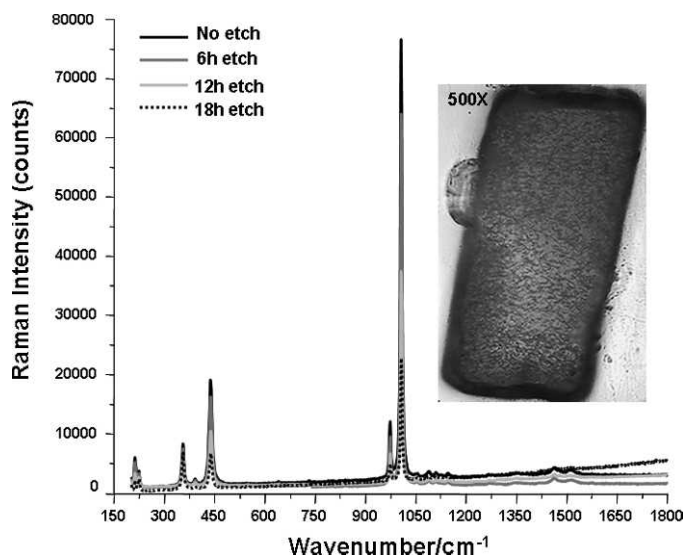


Fig. 1. *Homogeneous grain*: grain after 18 hours of etching with  $500\times$  nominal magnification (inset) and surface analyses using micro-Raman spectroscopy as a function of etching time.

TABLE I. Raman assignments for the zircon mineral.<sup>a</sup>

Raman (514.5 nm) (cm <sup>-1</sup> )	Assignments
356	(E <sub>g</sub> ) or SiO <sub>4</sub> ν <sub>4</sub>
393	(E <sub>g</sub> ) or (B <sub>1g</sub> )
439	SiO <sub>4</sub> ν <sub>2</sub> (A <sub>1g</sub> )
974	SiO <sub>4</sub> ν <sub>1</sub> (A <sub>1g</sub> )
1008	SiO <sub>4</sub> ν <sub>3</sub> (B <sub>1g</sub> )

<sup>a</sup> ν<sub>1</sub>, symmetric stretching; ν<sub>2</sub>, symmetric bending; ν<sub>3</sub>, antisymmetric stretching; ν<sub>4</sub>, antisymmetric bending; A<sub>1g</sub>, B<sub>1g</sub>, internal vibrational modes; E<sub>g</sub>, external modes

## RESULTS

**Micro-Raman Spectroscopy.** Figures 1, 2, and 3 present the Raman spectra for *homogeneous*, *anomalous*, and *hybrid* grains, respectively, whose optical images are given in figure insets. The assignments of the main Raman bands are given in Table I, which summarizes literature data.<sup>31,32</sup> The vibrational modes are related to Si–O bonding. Raman data (wavenumber, intensity, relative intensity, and full width at half-maximum (FWHM)) are shown in Table II.

**Homogeneous Grain.** The inset in Fig. 1 shows an optical image obtained with 500× nominal magnification and reveals a uniform density of fission tracks for a grain surface after 18 hours of etching. Four Raman spectra were collected over sequential etching times (without etching and with 6, 12, and 18 hours of etching, see Fig. 1). It can be seen that the absolute and relative intensity of the peaks decreases as etching time

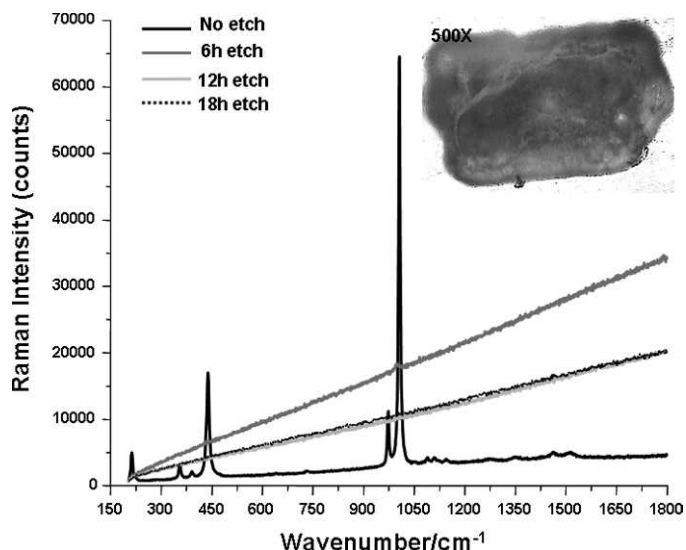


FIG. 2. *Anomalous grain*: grain after 18 hours of etching with 500× nominal magnification (inset) and surface analyses using micro-Raman spectroscopy as a function of etching time.

increases (Table II), but even after 18 hours of etching a significant percentage of the crystalline structure is maintained. The latter indicates that this type of grain is suitable for zircon FTM dating. The same analyses were done for other *homogeneous* grain areas and the results are similar. Similar results were also found for *heterogeneous* grains.<sup>27</sup> However,

TABLE II. Raman data (wavenumber, intensity, relative intensity, FWHM) for the natural zircon grains (JP sample), with and without chemical etching.<sup>a</sup>

Not-etched		Etched					
		6 hours		12 hours		18 hours	
$\bar{\nu}$ (cm <sup>-1</sup> )	Intensity [RI] (FWHM)	$\bar{\nu}$ (cm <sup>-1</sup> )	Intensity [RI] (FWHM)	$\bar{\nu}$ (cm <sup>-1</sup> )	Intensity [RI] (FWHM)	$\bar{\nu}$ (cm <sup>-1</sup> )	Intensity [RI] (FWHM)
<b>HOMOGENEOUS GRAINS</b>							
223.8	6123 [8.26%] (7.34)	224.1	5209 [7.03%] (7.63)	224	3865 [5.21%] (7.62)	223.5	2486 [3.35%] (7.88)
355.1	7937 [10.71%] (7.19)	355.5	7691 [10.38%] (7.21)	355.6	7201 [9.72%] (6.98)	355.5	6974 [9.41%] (7.14)
390.6	1703 [2.30%] (7.02)	390.5	1555 [2.10%] (7.11)	390.5	1346 [1.80%] (7.14)	390.5	1037 [1.4%] (7.29)
437.8	19463 [26.27%] (9.38)	438.1	17817 [24.05%] (9.41)	438.1	11549 [15.59%] (9.07)	437.9	6038 [8.15%] (8.92)
974.2	11449 [15.45%] (6.14)	974	10102 [13.63%] (6.56)	974.5	7641 [10.31%] (6.71)	974.3	4723 [6.37%] (6.67)
1006	74085 [100%] (5.94)	1006.5	62380 [84.20%] (6.04)	1006.6	37489 [50.60%] (5.69)	1006.5	22607 [30.51%] (5.63)
<b>ANOMALOUS GRAINS</b>							
224	5011 [7.81%] (7.44)	–	–	–	–	–	–
355.5	3297 [5.38%] (8.33)	–	–	–	–	–	–
390	1816 [2.97%] (8.42)	–	–	–	–	–	–
437	16920 [27.60%] (9.96)	–	–	–	–	–	–
975	9142 [14.90%] (6.65)	–	–	–	–	–	–
1007.3	61214 [100%] (6.75)	1005.7	1156 [1.89%] (11.40)	–	–	–	–
<b>HYBRID GRAINS – Area A</b>							
224	4911 [8.27%] (7.02)	224.2	4792 [8.07%] (7.24)	224.5	4255 [7.17%] (7.35)	224.5	3551 [5.98%] (7.42)
355.1	3844 [6.48%] (6.89)	355.1	3671 [6.18%] (6.92)	355.5	3288 [5.54%] (7.01)	355.5	2790 [4.70%] (7.13)
390.6	1476 [2.49%] (7.66)	391	1387 [2.33%] (7.85)	391	1002 [1.68%] (8.31)	391.2	833 [1.40%] (8.44)
437.8	14569 [24.55%] (9.41)	437.8	14023 [23.63%] (9.69)	437.8	10723 [18.07%] (9.98)	438.1	7610 [12.83%] (10.11)
974.2	7832 [13.19%] (6.02)	974.5	7534 [12.69%] (6.13)	974.5	4365 [7.35%] (6.26)	974.8	2968 [5.00%] (6.34)
1006.5	59354 [100%] (6.70)	1007.1	55263 [93.10%] (6.94)	1007.5	38452 [64.78%] (7.11)	1007.8	24199 [40.77%] (7.27)
<b>HYBRID GRAINS – Area B</b>							
224.5	5452 [8.92%] (7.59)	–	–	–	–	–	–
355	3877 [7.98%] (8.54)	–	–	–	–	–	–
390	1204 [1.97%] (9.61)	–	–	–	–	–	–
438.5	15798 [25.86%] (9.90)	438.6	2935 [4.80%] (12.48)	438.6	1129 [1.85%] (13.23)	–	–
975.3	6843 [11.20%] (7.25)	–	–	–	–	–	–
1007.7	61085 [100%] (6.73)	1006.9	7127 [11.7%] (10.35)	1007.8	1567 [2.56%] (8.9)	–	–

<sup>a</sup>  $\bar{\nu}$  is the Raman wavenumber, RI is the relative intensity regarding the 1008 cm<sup>-1</sup> peak, FWHM is the Full Width at Half Maximum (cm<sup>-1</sup>).

**TABLE III.** Main oxide chemical elements estimative obtained through SEM (EDS).

Grain classification	Areas	ZrO <sub>2</sub> (%)	SiO <sub>2</sub> (%)	HfO <sub>2</sub> (%)
<i>Homogeneous</i> (Fig. 4)	P1	67.75	30.25	2
	P2	67.49	30.52	1.99
	P3	67.37	30.53	1.92
<i>Anomalous</i> (Fig. 5)	P1	73.82	0.72	2.22
	P2	60.65	0.62	1.99
	P3	56.15	0.63	1.67
<i>Hybrid</i> (Fig. 6)	P1	68.13	30.8	1.07
	P3	67.94	30.55	1.5
	P4	67.69	30.62	1.69
	P5	68.52	29.96	1.52

because only about 10% of the grains we have so far analyzed in over 50 sedimentary samples from the Bauru Basin are of the *homogeneous* type, it is important to pursue other grain types that allow the use of FTM dating. A thorough counting performed of 500 grains from the Bauru Basin lead to the following proportions of grains: anomalous, 60%; hybrid, 20%; and heterogeneous, 10%. The cretaceous rocks from the Paraná Basin, where the Bauru Group is located, are composed predominantly of sandstones with different grain sizes (coarse, medium, fine, and very fine grained), colors (pale brown to reddish), and characteristics (conglomeratic, clay, mudstone). They present a mean uranium content of 150 ppm and mean Th/U ratio of 0.7. The grains described in this work (*homogeneous*, *anomalous*, and *hybrid*) are present both in the samples from the Bauru Group and from the Barreiras Formation (JP sample). The mean uranium content obtained for both suites of detrital zircon are: Bauru Group ~ 150 ppm and Barreiras Formation ~ 130 ppm (Table III).

**Anomalous Grain.** The inset in Fig. 2 shows an optical image obtained with 500× nominal magnification for an *anomalous* grain after 18 hours of etching. It is observed that the grain surface is totally damaged. Raman spectra were measured for the grain without etching and after 6, 12, and 18

hours of etching (Fig. 2). The crystallinity of the *anomalous* grains is more affected by etching than the crystallinity of *homogeneous* grains (Table II). The Raman spectra are already flattened in the first hours of etching, indicating that the grain crystalline structure is completely damaged. As mentioned in the Experimental Procedures section, this etching damage may be occurring due to several physicochemical phenomena, and not only due to metamictization. It is also possible to have incorporation of other minerals. Other grains of this kind were analyzed, showing similar results. Therefore, these grains cannot be used for FTM dating.

**Hybrid Grain.** The inset in Fig. 3 shows an optical image obtained with nominal magnification of 500× for a *hybrid* grain after 18 hours of etching. For this grain, fission tracks are uniformly distributed within certain areas (e.g., area A) while for other areas (e.g., area B) fission tracks are not observed. In both areas, Raman spectra were obtained for the grain without etching and after 6, 12, and 18 hours of etching (Fig. 3 and Table II). The *hybrid* grain can be interpreted as a mixture of the *homogeneous* and *anomalous* grains. Area A presents a similar trend (Raman data) to that found for the *homogeneous* grains, i.e., a significant portion of the surface and mineral crystalline structure is preserved. On the other hand, in area B, the results are similar to those found for *anomalous* grains, i.e., loss of crystalline structure during the first hours of etching. Other grains of this type were analyzed showing similar results. This trend indicates that, if at least one area with uniform density is found (*hybrid* grain area A), then the *hybrid* grains could be used for FTM through the external detector method.

**Scanning Electronic Microscopy.** The SEM (EDS) analyses were carried out for *homogeneous*, *anomalous*, and *hybrid* grains in order to qualitatively investigate their chemical composition. The analyses of SEM (EDS) were done on the same grains used to obtain the micro-Raman spectroscopy after 18 hours of etching.

**Homogeneous Grain.** An SEM (back-scattered electron, BSE) image and an estimate of the main chemical oxide elements (ZrO<sub>2</sub>, SiO<sub>2</sub>, and HfO<sub>2</sub>) obtained through SEM (EDS) for a *homogeneous* grain are shown in Fig. 4A and Table III,

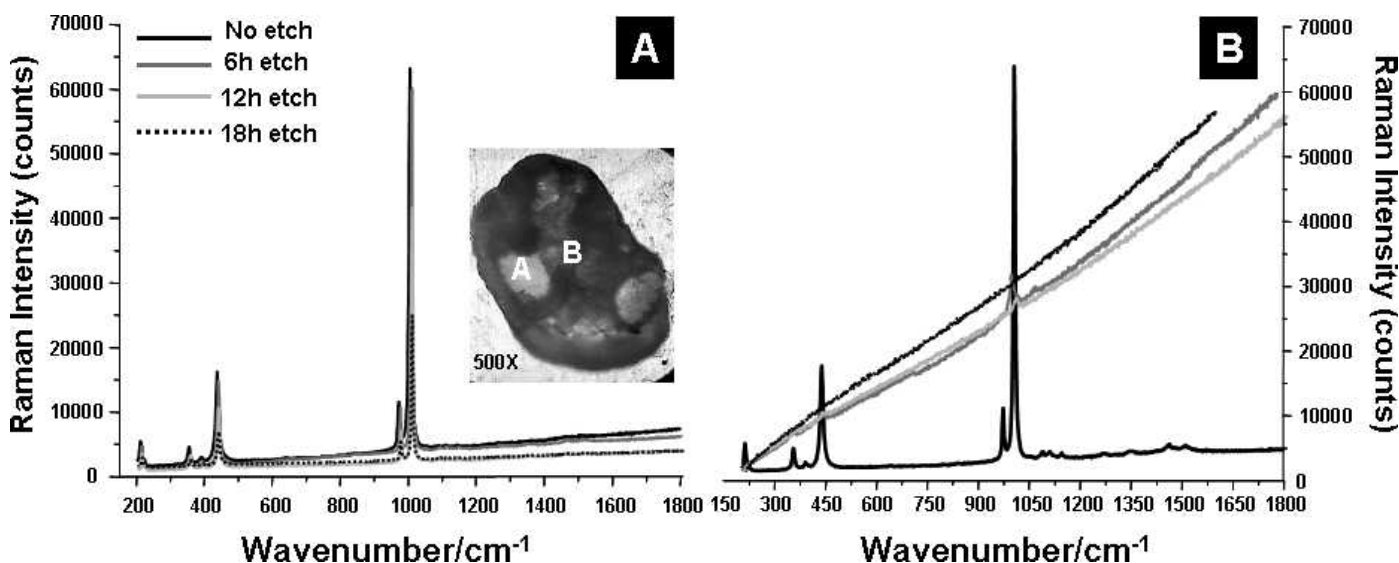


FIG. 3. *Hybrid grain*: grain after 18 hours of etching with 500× nominal magnification (inset) and surface analyses using micro-Raman spectroscopy as a function of etching time in areas A and B.

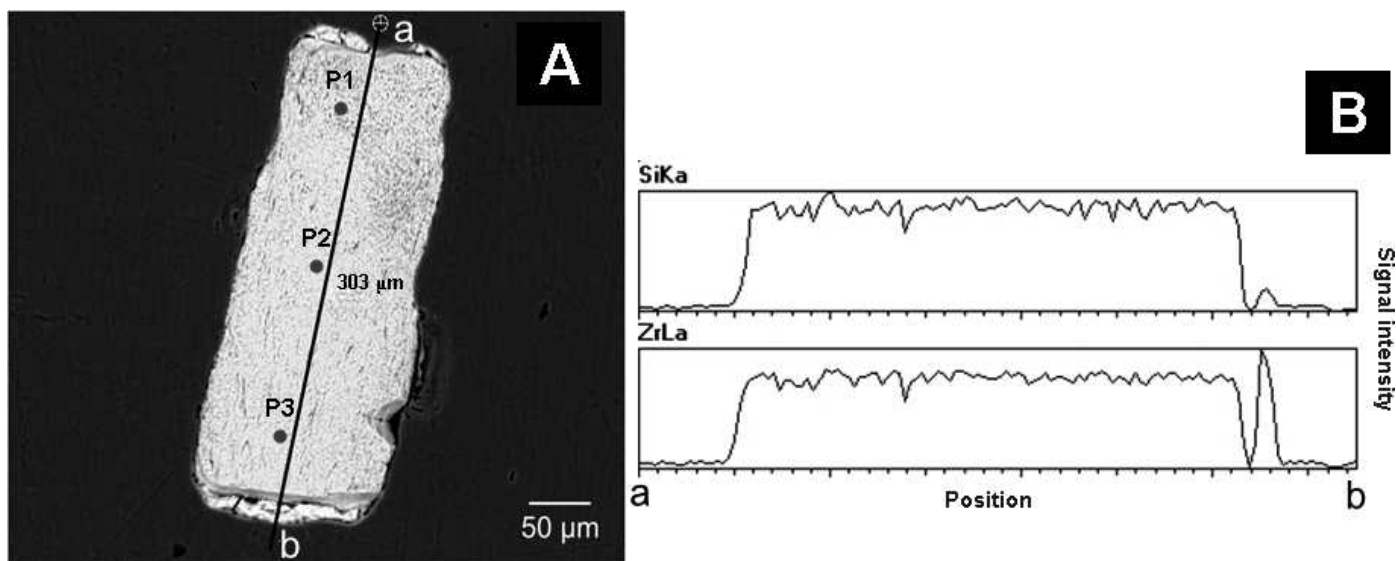


FIG. 4. *Homogeneous grain*: (A) SEM (BSE) grain image after 18 hours of etching and (B) SEM (EDS) line profile analysis.

respectively. The chemical analysis was done in three different areas, approximately in the same areas used to record the micro-Raman spectra. A SEM (EDS) line profile analysis was also done and the result is shown in Fig. 4B. Table III shows that the measurements of  $ZrO_2$ ,  $SiO_2$ , and  $HfO_2$  in three different areas agree with natural zircon (e.g., sample 4403 from Sri Lanka: 67.8%  $ZrO_2$ ; 32.0%  $SiO_2$ ; and 0.95%  $HfO_2$ ).<sup>24</sup> The line profile (Fig. 4B) shows that zirconium and silicon measurements are uniform in the whole grain. In this kind of grain, even after 18 hours of etching, the crystallinity could be verified by micro-Raman spectroscopy (Fig. 1). It is worth noting that non-standard zircon<sup>27</sup> also presented similar main chemical oxide elements and micro-Raman spectra.

**Anomalous Grain.** Figure 5A shows a SEM (BSE) image of an *anomalous* grain damaged due to the chemical etching. Table III shows the quantity of  $ZrO_2$ ,  $SiO_2$ , and  $HfO_2$  obtained in three areas of the grain. This grain is different from the one

used in the micro-Raman spectroscopy measurement (Fig. 2) because background noise during the SEM measurements prevented the EDS analysis. Instead, another anomalous grain was chosen and characterized. Because the anomalous grains present similar characteristics, the final result was not changed. The values obtained from this analysis were not in accordance with the chemical composition of standard zircon. It can be seen in Fig. 5B that the SEM (EDS) line profile shows a greater change of the zirconium and silicon amount in this grain than in the *homogeneous* grain. Also, from Table III, a drastic decrease in  $SiO_2$  can be seen, reaching almost null concentration. The amount of  $ZrO_2$  varies, usually also decreasing. However, the latter variation is much smaller than the former. With these observations, it could be possible to conclude that the zircon crystallinity depends on the amount of silicon. This crystallinity loss could also be observed in the micro-Raman spectra evolution (Fig. 2).

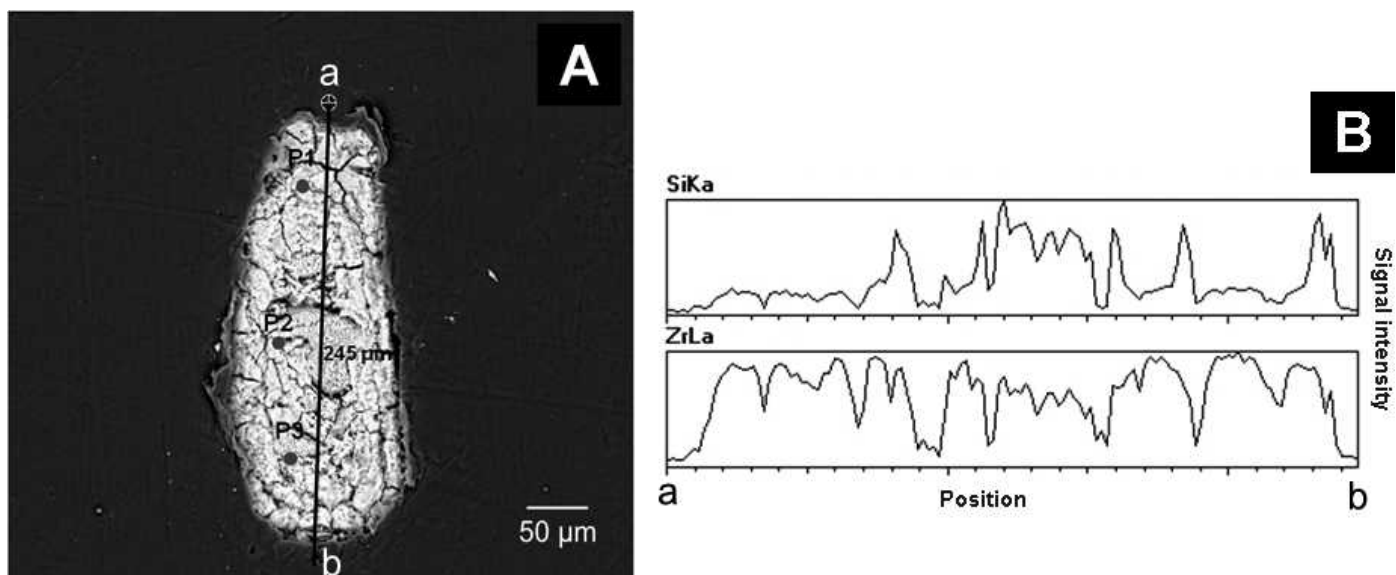


FIG. 5. *Anomalous grain*: (A) SEM (BSE) grain image after 18 hours of etching and (B) SEM (EDS) line profile analysis.

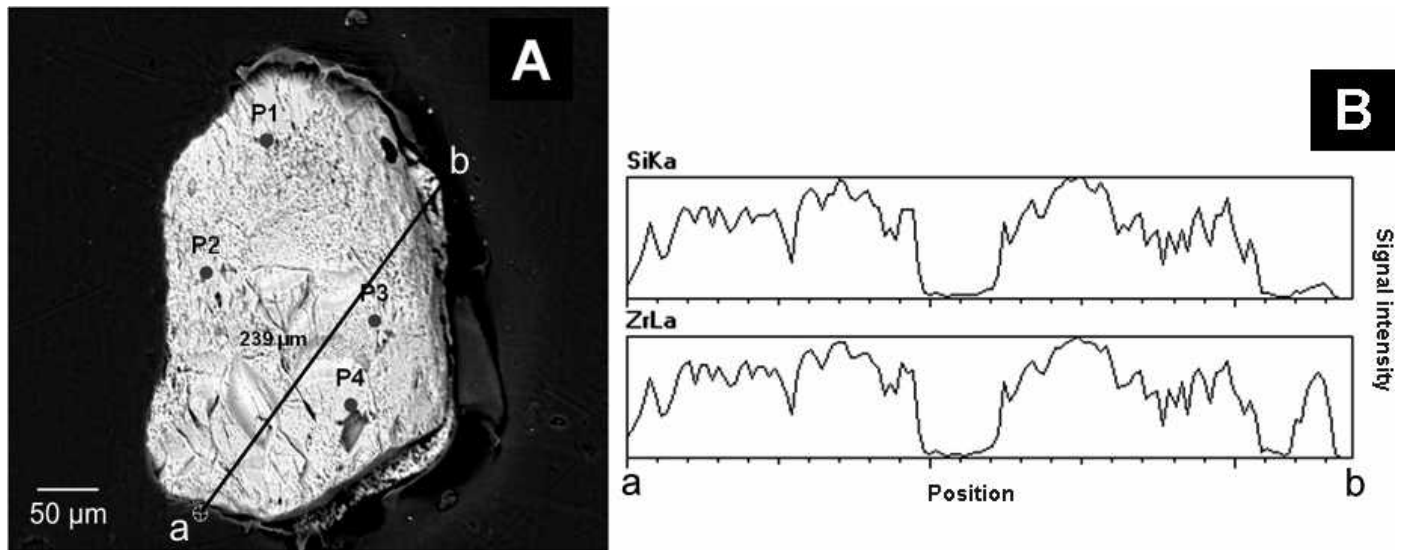


FIG. 6. *Hybrid grain*: (A) SEM (BSE) grain image after 18 hours of etching and (B) SEM (EDS) line profile analysis.

**Hybrid Grain.** A SEM (BSE) image of a *hybrid* grain is presented in Fig. 6A. In this grain the analysis of the main chemical oxide elements was carried out in four areas using SEM (EDS). The results are shown in Table III. It can be seen that the values of ZrO<sub>2</sub> and SiO<sub>2</sub> are similar to those of standard zircon. These areas can be related to the presence of uniform fission track density. Micro-Raman spectra indicated the existence of crystallinity for these areas even after 18 hours of etching (Fig. 3A). So, these areas could be used for FTM dating through the external detector method. On the other hand, the SEM (EDS) line profile analysis (Fig. 6B) shows areas that have different characteristics compared to *homogeneous* grains (Fig. 4B). It is important to observe an almost null value for SiO<sub>2</sub> and ZrO<sub>2</sub> in certain areas. These areas can be related to a totally damaged surface (like the *anomalous* grain). The presence of totally damaged areas does not prohibit the utilization of the hybrid grains for FTM, since it is possible to work within the homogeneous areas.

**Fission Track Method and U-Pb in Situ Dating.** As an example, eight zircon grains from Barreiras Formation (JP sample), near the city of Mataraca, State of Paraíba, Brazil, are shown in Table IV. These grains were dated by both FT and U-Pb dating methods. The U/Pb ages were obtained by aiming the laser at the areas where fission tracks were developed, which improved the agreement of the obtained U/Pb ages (Table IV). The ages obtained by FTM in homogeneous and hybrid grains are consistent. As also shown in Table IV, the ages found using the U-Pb method are systematically higher than those found via FTM. The latter is also consistent since the closure temperature for the U-Pb system is approximately 700 °C and for zircon FTM is approximately 240 °C.<sup>30</sup> The FTM dating data strengthen the conclusion that the *hybrid* grains can be used in FTM analyses. Further dating data and more details about geological interpretations are beyond the scope of this article and might be subjects of future research.

TABLE IV. Zircon U-Pb and FTM data for JP sample.<sup>a</sup>

Grain #	LA-MC-ICP-MS DATA								AGES (Ma)								
			Ratios #				FTM DATA				U-Pb in situ		FTM				
	<sup>232</sup> Th/ <sup>238</sup> U	U (ppm)	<sup>207</sup> Pb/ <sup>235</sup> U	± σ (%)	<sup>206</sup> Pb/ <sup>238</sup> U	± σ (%)	<sup>207</sup> Pb/ <sup>206</sup> Pb	± σ (%)	ρ <sub>s</sub> × 10 <sup>7</sup> cm <sup>-2</sup>	N <sub>s</sub>	ρ <sub>i</sub> × 10 <sup>6</sup> cm <sup>-2</sup>	N <sub>i</sub>	(± 2σ)	% Conc	(± 2σ)		
2 [B1]	0.49	115.8	11.70205	0.68	0.47702	0.44	0.17792	0.52	2.85	73	0.923	30	2634	17	95	371	80
3 [B3]*	0.88	76.0	0.82775	3.53	0.09963	1.71	0.06026	3.09	3.39	130	1.323	43	612	20	100	373	80
8 [C3]*	0.78	45.0	3.87207	2.24	0.28044	0.98	0.10014	2.01	2.63	118	1.931	63	1597	26	98	346	72
10 [D7]	0.66	87.7	6.52885	1.39	0.37460	0.86	0.12641	1.09	3.56	114	1.204	39	2050	24	100	356	79
11 [D9]*	1.01	33.3	3.60351	2.85	0.26737	1.26	0.09775	2.56	3.03	97	1.441	47	1533	32	97	319	67
17 [F3]*	0.80	110.3	6.41747	1.37	0.36455	0.93	0.12767	1.00	2.92	112	2.002	29	2066	36	97	353	73
23 [G6]	1.32	39.4	3.79171	2.53	0.27693	1.38	0.09931	2.12	2.86	28	1.052	38	1582	35	98	342	72
28 [H6]*	0.42	112.9	9.09817	1.09	0.41532	0.51	0.15888	0.97	3.27	48	0.593	38	2444	33	92	365	76

<sup>a</sup> The U-Th-Pb ages (concordant ages) are calculated after Ludwig program for those zircons with discordance <10%; Sample and standard are corrected after Pb and Hg blanks; <sup>206</sup>Pb/<sup>207</sup>Pb and <sup>206</sup>Pb/<sup>238</sup>U are corrected after common Pb presence; Common Pb assuming <sup>206</sup>Pb/<sup>238</sup>U and <sup>207</sup>Pb/<sup>235</sup>U concordant age; <sup>235</sup>U = 1/137.88\*U<sub>total</sub>; Standard GJ-1; Th/U = <sup>232</sup>Th/<sup>238</sup>U\*0.992743; the isotope ratios errors in the table are calculated with 1σ and the age with 2σ error; otherwise the concordant age is after <sup>207</sup>Pb/<sup>206</sup>Pb age. ρ<sub>s</sub> (ρ<sub>i</sub>), spontaneous (induced) track density; N<sub>s</sub> (N<sub>i</sub>), number of tracks counted to determine ρ<sub>s</sub> (ρ<sub>i</sub>); ρ<sub>i</sub>, induced track density was measured in muscovite mica acting as an external detector (EDM). The grains with \* are examples of *hybrid* grains.

## CONCLUSION

Three types of zircon grains were identified according to the way they react to chemical etching. After being analyzed through optical microscopy, micro-Raman spectroscopy, and SEM they were classified as *homogeneous*, *anomalous*, and *hybrid* grains. After etching, the *homogeneous* grains have their crystal lattice slightly altered and present a uniform fission-track distribution. The *anomalous* grains surfaces are strongly etching-damaged just after the first hours of etching and accordingly do not reveal fission tracks. On the other hand, the *hybrid* grains present a special characteristic: after the etching procedure some grain areas have no crystalline structure (as the *anomalous* grains), while other areas of the same grain reveal fission tracks (as the *homogeneous* grains).

The results obtained through micro-Raman spectroscopy (as a function of etching time) and SEM (EDS) analyses on the zircon surface indicated that areas with standard main oxide element concentrations and characteristic Raman spectra present a uniform fission track density, which can be used for FTM dating (through the external detector method). In other words, the areas that could reveal fission tracks are essentially zircon. In this way, not only *homogeneous* grains but also *hybrid* grains can be used for dating purposes. This result is very important for FTM because in many cases the natural zircon samples, after the etching procedure, have been damaged. Using the *hybrid* grains as well will increase the statistics of the analysis significantly. An interesting result obtained in this work is that in the case of the *anomalous* grains there is an accentuated reduction of the silicon oxide content, which may indicate the influence of the silicon in the structural stability of the mineral.

## ACKNOWLEDGMENTS

The authors are grateful to Professor Giulio Bigazzi and Professor John Garver for providing several sheets of teflon PFA and to an unknown referee for his very helpful comments. We also are grateful to Brazilian foundations FAPESP (Fundação de Amparo à Pesquisa do Estado de São Paulo), CAPES (Coordenação de Aperfeiçoamento de Pessoal de Nível Superior), and CNPq (Conselho Nacional de Desenvolvimento Científico e Tecnológico), which financially supported this work, and to the IPEN/CNEN – São Paulo for providing the neutron irradiations.

1. K. Gallagher, R. Brown, C. Johnson. "Fission Track Analysis and Its Applications to Geological Problems". *Annu. Rev. Earth Planet. Sci.* 1998. 26(1): 519–572.
2. T. Tagami. "Zircon Fission-Track Thermochronology and Applications to Fault Studies". *Rev. Mineral. Geochem.* 2005. 58(1): 95–122.
3. M. Murakami, J. Kosler, H. Takagi, T. Tagami. "Dating pseudotachylite of the Auke Shear Zone using zircon fission-track and U–Pb methods". *Tectonophys.* 2006. 424(1-2): 99–107.
4. R. Yamada, T. Tagami, S. Nishimura, H. Ito. "Annealing kinetics of fission tracks in zircon: an experimental study". *Chem. Geol. (Isot. Geosci. Sect.)*. 1995. 122(1-4): 249–258.
5. T. Tagami, A. Carter, A.J. Hurford. "Natural long-term annealing of the zircon fission-track system in Vienna Basin deep borehole samples: constraints upon the partial annealing zone and closure temperature". *Chem. Geol. (Isot. Geosci. Sect.)*. 1996. 130(1-2): 147–157.
6. M. Murakami, K. Yamada, T. Tagami. "Short-term annealing characteristics of spontaneous fission tracks in zircon: A qualitative description". *Chem. Geol., (Isot. Geosci. Sect.)*. 2006. 227(3-4): 214–222.
7. S. Guedes, J. Hadlern, P.J. Iunes, K.M.G. Oliveira, P.A.F.P. Moreira, and C.A. Tellos. "Kinetic model for the annealing of fission tracks in zircon". *Radiat. Meas.* 2005. 40(2-6): 517–521.
8. J.I. Garver. "Etching zircon age standards for fission-track analysis". *Radiat. Meas.* 2003. 37(1): 47–53.
9. G. Wagner, P. van den Haute. *Fission-track Dating*. Kluwer Academic: Norwell, 1992. 6th vol., pp. 285.
10. E. Balan, D.R. Neuville, P. Trocellier, E. Fritsch, J.P. Muller, G. Calas. "Metamictization and chemical durability of detrital zircon". *Am. Mineral.* 2001. 86(9): 1025–1033.
11. C.S. Palenik, L. Nasdala, R.C. Ewing. "Radiation damage in zircon." *Am. Mineral.* 2003. 88(5-6): 770–781.
12. L. Nasdala, G. Irmer, D. Wolf. "The degree of metamictization in zircons: a Raman spectroscopic study". *Eur. J. Mineral.* 1991. 7: 471–478.
13. L. Nasdala, M. Wenzel, G. Vavra, G. Irmer, T. Wenzel, B. Kober. "Metamictisation of natural zircon: accumulation versus thermal annealing of radioactivity-induced damage". *Contr. Min. Petr.* 2001. 141(2): 125–144.
14. M. Zhang, E.K.H. Salje, I. Farnan, A. Graeme-Barber, P. Daniel, R.C. Ewing, A.M. Clark, H. Leroux. "Metamictization of zircon: Raman spectroscopic study". *J. Phys.: Condens. Matter.* 2000. 12(8): 1915–1925.
15. M. Lodzinski, R. Wrzalik, M. Sitarz. "Micro-Raman spectroscopy studies of some accessory minerals from pegmatites of the Sowie Mts and Strzegom-Sobótka massif, Lower Silesia, Poland". *J. Mol. Struct.* 2005. 744: 1017–1026.
16. H.D. Holland, D. Gottfried. "The effect of nuclear radiation on the structure of zircon". *Acta Cryst.* 1955. 8(6): 291–300.
17. P.J. Wasilewski, F.E. Senftle, J.E. Vaz, A.N. Thorpe, C.C. Alexander. "A study of the natural  $\alpha$ -recoil damage in zircon by infrared spectra". *Radiat. Eff.* 1973. 17(3-4): 191–199.
18. E.K.H. Salje, J. Chrosch, R.C. Ewing. "Is "metamictization" of zircon a phase transition?" *Am. Miner.* 1999. 84(7-8): 1107–1116.
19. S. Ríos, E.K.H. Salje, M. Zhang, R.C. Ewing. "Amorphization in zircon: evidence for direct impact damage". *R.C. J. Phys.: Cond. Matter.* 2000. 12(11): 2401–2412.
20. K.T. Trachenko, M.T. Dove, E. Salje. "Modelling the percolation-type transition in radiation damage". *J. Appl. Phys.* 2000. 87(11): 7702–7707. 2000.
21. B.C. Chakoumakos, T. Murakami, G.R. Lumpkin, R.C. Ewing. "Alpha-Decay-Induced Fracturing in Zircon: The Transition from the Crystalline to the Metamict State". *Science.* 1987. 236(4808): 1556–1559.
22. A.C. McLaren, J.D. Fitz Gerald, I.S. Williams. "The microstructure of zircon and its influence on the age determination from Pb/U isotopic ratios measured by ion microprobe". *Geochim. Cosmochim. Acta.* 1994. 58(2): 993–1005.
23. L. Nasdala, R.T. Pidgeon, D. Wolf, G. Irmer. "Metamictization and U-PB isotopic discordance in single zircons: a combined Raman microprobe and SHRIMP ion probe study". *Mineral. and Petrol.* 1998. 62(1-2): 1–27.
24. T. Geissler, H. Schleicher. "Improved U–Th–total Pb dating of zircons by electron microprobe using a simple new background modeling procedure and Ca as a chemical criterion of fluid-induced U-Th-Pb discordance in zircon". *Chem. Geol.* 2000. 163(1-4): 269–285.
25. G.R. Lumpkin. "Alpha-decay damage and aqueous durability of actinide host phases in natural systems". *J. Nucl. Mater.* 2001. 289(1-2): 136–166.
26. V.D. Araújo, Y.A. Reyes-Peres, R.O. Lima, A.P. Pelosi, L. Menezes, V.C. Córdoba, F.P. Lima-Filho, *Geol. USP Sér. Cient.* 2006. 6(2): 43–49, in Portuguese.
27. A.N.C. Dias, C.A. Tello Saenz, C.J.L. Constantino, C.J. Soares, F.P. Novaes, A.M.O.A. Balan. *J. Raman Spectrosc.* 2009. 40(1): 101–106.
28. M. Menneken, A.A. Nemchin, T. Geisler, R.T. Pidgeon, S.A. Wilde. "Hadean diamonds in zircon from Jack Hills, Western Australia". *Nature.* 2007. 448(7156): 917–920.
29. C.W. Passchier, R.A.J. Trouw. *Micro-tectonics*. New York: Springer, 2005. 2nd ed., pp. 366.
30. M.T. Brandon, M.K. Roden-Tice, J.I. Garver. "Late Cenozoic exhumation of the Cascadia accretionary wedge in the Olympic Mountains, northwest Washington State". *Bull. Geol. Soc. Am.* 1998. 110(8): 985–1009.
31. T. Geisler, R.T. Pidgeon, W. van Bronswijk, R. Kurtz. "Transport of uranium, thorium, and lead in metamict zircon under low-temperature hydrothermal conditions". *Chem. Geol. (Isot. Geosci. Sect.)*. 2002. 191(1-3): 141–154.
32. L. Nasdala, M. Zhang, U. Kempe, G. Panczer, M. Gaft, M. Andrut, M. Ploetze. "Spectroscopic methods applied to zircon". *Rev. Mineral. Geochem.* 2003. 53(1): 427–467.